Research Square

Preprints are preliminary reports that have not undergone peer review.
They should not be considered conclusive, used to inform clinical practice,
or referenced by the media as validated information.

Virome-Wide Antibody Signatures Are Associated with a Persistent High-CD8⁺ T-Cell Phenotype in Immune-Reconstituted Individuals with HIV

Zhongyi Zhang
Capital Medical University
Guoli Li
Capital Medical University
Hui Liu
Capital Medical University
Chuan Song
Capital Medical University
Huan Liu
Capital Medical University
Danying Chen
Capital Medical University
Rui Qiao
Peking University Ditan Teaching Hospital
Shuna Zhang
Peking University Ditan Teaching Hospital
Yinghui Gao
Capital Medical University
Yujiao Duan
Capital Medical University
Xuesen Zhao
Capital Medical University
Xin Li
leaxin@ccmu.edu.cn

Capital Medical University

Article

Keywords: HIV, CD8-positive T lymphocytes, antibody repertoire, phage immunoprecipitation sequencing, immune reconstitution

Posted Date: November 25th, 2026

DOI: https://doi.org/10.21203/rs.3.rs-11687281/v1

License: This work is licensed under a Creative Commons Attribution 4.0 International License.
Read Full License

Additional Declarations: No competing interests reported.

Title Page

Manuscript type: Research article

Title: Virome-Wide Antibody Signatures Are Associated with a Persistent High-CD8$^+$ T-Cell Phenotype in Immune-Reconstituted Individuals with HIV

Authors: Zhongyi Zhang[1,#], Guoli Li[1,2,3,4,#], Hui Liu[1], Chuan Song[1,2,3,4], Huan Liu[1,2,3,4], Danying Chen[1,2,3,4], Rui Qiao[5], Shuna Zhang[5], Yinghui Gao[1], Yujiao Duan[1], Xuesen Zhao[1,2,3,4,5,*], Xin Li[1,5,*]

Affiliations:

1. National Center for Infectious Diseases, Beijing Ditan Hospital, Capital Medical University, Beijing 100015, China.

2. National Key Laboratory of Intelligent Tracking and Forecasting for Infectious Diseases, Beijing Ditan Hospital, Capital Medical University, Beijing 100015, China.

3. Beijing Key Laboratory of Viral Infectious Disease, Institute of Infectious Diseases, Beijing Ditan Hospital, Capital Medical University, Beijing 100015, China.

4. Beijing Institute of Infectious Diseases, Beijing 100015, China.

5. Center of Integrated Traditional Chinese and Western Medicine, Peking University Ditan Teaching Hospital, Beijing 100015, China.

***Corresponding authors:** Xin Li, PhD, and Xuesen Zhao, PhD, National Center for Infectious Diseases, Beijing Ditan Hospital, Capital Medical University, No. 8 Jingshun East Street, Chaoyang District, Beijing 100015, China. Email: leaxin@ccmu.edu.cn (X.L.); zhaoxuesen@ccmu.edu.cn (X.Z.).

# Zhongyi Zhang and Guoli Li contributed equally to this work.

Tables and figures: 2 main tables; 6 main figures; 1 supplementary table; 5 supplementary figures

Prior presentation/preprint: None.

Author declaration: All authors have reviewed and approved the submitted manuscript, meet authorship criteria, and consider the work to represent honest and accurate research.

Abstract

Background: Antiviral antibody profiles remain incompletely characterized in people with HIV who achieve $CD4^+$ T-cell recovery and sustained virologic suppression. We used phage immunoprecipitation sequencing (PhIP-seq) to examine these profiles and their associations with longitudinal T-cell measurements.

Methods: We profiled 38 CRs and 38 age- and sex-matched HIV-negative controls (NCs) using PhIP-seq and integrated antibody profiles with longitudinal T-cell measurements.

Results: CRs had higher total virscores and 34 differential antibody-reactive peptides versus NCs, including 33 HIV-1 peptides and one Epstein-Barr virus (EBV) peptide. An exploratory $CD8^+$ threshold stratified CRs into CD8-high and CD8-low subgroups. CD8-high CRs maintained higher longitudinal $CD8^+$ T-cell counts despite similar sampling-time $CD4^+$ T-cell counts and showed 74 differential peptides versus NCs. These included 40 newly identified differential peptides, 19 of which were derived from non-HIV viruses, including cytomegalovirus, EBV, pseudocowpox virus, herpes simplex virus types 1 and 2, macacine alphaherpesvirus 1, salivirus A, and salivirus FHB. The relationship between Env recognition and evolutionary rate differed between CD8 subgroups.

Conclusions: Virome-wide antibody profiling identified an immunologically distinct subgroup of individuals with HIV, characterized by persistent $CD8^+$ T-cell elevation and broader HIV and non-HIV antibody recognition despite sustained virologic suppression and $CD4^+$ T-cell recovery. These findings support using routinely available $CD8^+$ T-cell counts to refine clinical stratification beyond conventional $CD4^+$ recovery criteria, identifying individuals with residual immune differences for continued immunologic assessment and surveillance.

Keywords: HIV; CD8-positive T lymphocytes; antibody repertoire; phage immunoprecipitation sequencing; immune reconstitution

Background

Antiretroviral therapy (ART) has transformed HIV infection from a progressive immunodeficiency into a manageable chronic disease, with durable viral suppression and recovery of $CD4^+$ T-cell counts serving as the principal markers of successful immune reconstitution [1]. Individuals who fail to achieve adequate $CD4^+$ T-cell recovery despite virologic suppression are commonly referred to as immunological non-responders (INRs). Most studies of immune reconstitution in treated HIV infection have focused on INRs and the mechanisms underlying inadequate $CD4^+$ T-cell recovery, whereas individuals with successful $CD4^+$ T-cell recovery have commonly served as reference populations [2,3]. Consequently, comparatively little attention has been paid to the immunologic heterogeneity that may persist among individuals with apparently successful immune recovery. In a recent analysis of 315,109 participants from the China National ART Cohort who initiated ART with $CD4^+$ T-cell counts <350 cells/μL and achieved virologic suppression at year 5, 35.5% had achieved $CD4^+$ T-cell counts ≥500 cells/μL [4]. A $CD4^+$ T-cell count ≥500 cells/μL during virologic suppression has been used to define complete immune recovery or restoration [5,6]. Nevertheless, recovery of $CD4^+$ T-cell counts does not necessarily indicate complete normalization of the immune system. Persistent abnormalities in $CD8^+$ T cells, CD4/CD8 ratios, immune activation, senescence, and inflammatory pathways have been reported even after $CD4^+$ T-cell counts recover to ≥500 cells/μL [7-10]. Thus, individuals with apparently complete immune reconstitution may remain immunologically heterogeneous, while their humoral immune status has received particularly limited attention.

In people with HIV, recurrent viral and opportunistic infections can shape antiviral humoral responses and leave persistent immune imprints reflected in the antibody repertoire. PhIP-seq, including the VirScan platform, combines phage display with high-throughput sequencing to interrogate antibody binding to thousands of linear viral peptides simultaneously; virome-wide

libraries further permit antibody responses to hundreds of human viruses to be assessed in parallel [11,12]. Larman and colleagues have applied this approach to HIV infection. These studies characterized the longitudinal evolution of HIV-specific antibody responses, compared antibody profiles among HIV controllers and individuals with treatment-induced viral suppression, and identified HIV antibody targets associated with viral load and spontaneous viremic control [13-16]. However, these investigations focused primarily on HIV-specific peptide recognition and virologic phenotypes. Systematic characterization of non-HIV antiviral antibody repertoires in treated people with HIV remains limited, and virome-wide antibody profiles have rarely been integrated with longitudinal cellular immune measurements. In particular, whether individuals who have already achieved sustained viral suppression and complete $CD4^+$ T-cell recovery nevertheless retain distinct virome-wide antibody signatures remains unknown.

Whereas the critical role of $CD4^+$ T cells in supporting humoral immune responses is well established [17], the association between the $CD8^+$ T-cell compartment and antiviral antibody responses, particularly in people with HIV, remains less well characterized. $CD8^+$ T cells may provide an important clinical link to this unresolved humoral heterogeneity. Interestingly, $CD8^+$ T-cell counts frequently remain elevated after years of suppressive ART, and persistent $CD8^+$ T-cell expansion or failure of CD4/CD8 ratio normalization has been associated with immune activation, senescence, inflammatory abnormalities, and adverse immune phenotypes even when $CD4^+$ T-cell counts have recovered [7-10]. Persistent or recurrent antigenic stimulation may contribute to this phenotype. For example, cytomegalovirus (CMV) coinfection has been linked to $CD8^+$ T-cell expansion and elevated CMV-specific antibody responses during suppressive ART [18,19]. These observations raise the possibility that persistent abnormalities in the $CD8^+$ T-cell compartment and enhanced antiviral antibody reactivity may represent complementary manifestations of cellular and humoral immunity after successful ART.

In this study, we investigated CRs, defined as individuals with a current $CD4^+$ T-cell count ≥500 cells/μL and plasma HIV RNA <50 copies/mL maintained for at least 3 years. By integrating virome-wide PhIP-seq with longitudinal $CD4^+$ and $CD8^+$ T-cell measurements, we examined whether CRs remained heterogeneous in their antiviral antibody repertoires and whether such heterogeneity was associated with persistent differences in cellular immune recovery. We found that virome-wide antibody signatures were associated with a persistent high-$CD8^+$ T-cell phenotype among CRs, characterized by broader HIV and non-HIV antibody recognition, abnormally elevated $CD8^+$ T-cell counts, and a distinct longitudinal $CD8^+$ T-cell trajectory. These findings suggest that conventional $CD4^+$ T-cell recovery and virologic suppression do not fully capture the immunologic heterogeneity that persists after successful ART.

Methods

Study design, participants, and clinical definitions

We conducted a retrospective observational study integrating longitudinal clinical records with cross-sectional antibody profiling at a tertiary HIV care center in Beijing, China. The source clinical cohort comprised 2,919 ART-treated people with HIV. Screening yielded 2,805 individuals meeting the broader immune-responder criteria used in the source cohort, and stored blood specimens collected between January and June 2025 were available for 183 individuals. For the present study, CRs were required to be aged 30-60 years and have complete longitudinal data, a current $CD4^+$ T-cell count ≥500 cells/μL [5,6], and sustained plasma HIV RNA <50 copies/mL for at least 3 years. Thirty-eight CRs met these criteria.

NCs were matched to CRs by sex and age within 3 years. NCs were excluded for active or chronic inflammatory disease, malignancy, rheumatic or autoimmune disease, or current immunosuppressive therapy. Thirty-eight NCs were included. All 76 participants were men, reflecting the available matched biospecimen pool. The study flow is shown in Figure 1A.

Baseline $CD4^+$ T-cell count and plasma HIV RNA were defined using measurements obtained before ART initiation. Current $CD4^+$ and $CD8^+$ T-cell counts were the measurements closest to plasma sampling for PhIP-seq. Longitudinal $CD4^+$ T-cell measurements for the overall CR cohort were summarized by calendar year for Figure 1B. For CD8-defined subgroup analyses, longitudinal $CD4^+$ and $CD8^+$ T-cell measurements were aligned by years since HIV diagnosis, calculated from the calendar year of each measurement relative to the diagnosis year. CD8-defined subgrouping was performed using the exploratory data-derived threshold described below.

Peripheral blood for PhIP-seq was collected between January and June 2025. Plasma was separated promptly, aliquoted, stored at −80°C, and handled using the same procedures across study groups before antibody profiling.

Virome-wide PhIP-seq profiling

Antiviral antibody reactivity was profiled with a T7 bacteriophage display library containing 122,602 peptides derived from more than 260 viruses known to infect humans [11,12]. Viral proteins were represented as 56-amino-acid peptides with 28-amino-acid overlaps. Peptide sequences were reverse-translated and codon-optimized for expression in Escherichia coli. Oligonucleotides were synthesized and cloned into the T7Select 10-3 system according to the manufacturer's instructions.

Plasma was incubated with the phage library overnight at 4°C. Protein A/G magnetic beads (40 µL; Tiandi Renhe, Beijing, China) were added, and incubation continued for 4 hours at 4°C, followed by three washes with Tris-buffered saline containing Tween 20. Bead-associated phage DNA underwent two rounds of polymerase chain reaction to add sequencing adapters and sample indices. Libraries were sequenced as 150-bp paired-end reads on an Illumina platform to a target depth of approximately 4 million reads per sample.

Raw reads underwent quality assessment and processing using fastp, Cutadapt, SeqKit, and BWA [20-23]. Reads exactly 168 bp long were retained after adapter processing, translated sequences containing premature stop codons were excluded, and nucleotide reads were aligned to the custom oligonucleotide reference. Probe-assigned reads were counted to generate the peptide-count matrix. Probe counts were converted to normalized read counts (NR). For each peptide, enrichment factor (EF) was calculated as NR in the plasma immunoprecipitation divided by NR in the corresponding mock-immunoprecipitation reference. A generalized Poisson model was used in the underlying PhIP-seq pipeline to estimate peptide-level enrichment significance. For downstream analyses, peptide-sample pairs meeting the enrichment criterion retained their measured EF values, whereas nonpositive pairs were assigned EF=1; accordingly, EF>1 denoted a positive peptide-sample pair.

Antibody repertoire analyses and cross-library assessment

Virscore was calculated for each participant and viral species. Positive peptides assigned to the same species were considered redundant when they shared a contiguous sequence of at least 7 amino acids; each redundant group was counted once [11]. Total virscore was the sum of species-level nonredundant reactivity. Peptide-level comparisons used the EF analysis matrix. HIV-derived peptides were mapped to annotated HIV-1 proteins and genomic positions.

To assess cross-library concordance, we used an independently designed UniRef90 library containing 1,120 64-amino-acid peptides derived from 54 viruses. The 34 virus-library peptides showing differential reactivity between CRs and NCs were paired with their closest sequence matches in the UniRef90 library. Amino-acid sequence identity was calculated for each pair. EF values for matched peptides were compared across the same 76 participants using Pearson correlation, and sequence identity was related to the corresponding cross-library correlation coefficient. Multiple virus-library peptides could map to the same UniRef90 peptide; this

171 analysis assessed cross-library measurement concordance rather than validation in independent
172 participants.

173 **Exploratory CD8 stratification and classification analyses**

174 Within CRs, associations between 571 HIV-derived peptide measures and five clinical variables
175 (current $CD8^+$ T-cell count, current $CD4^+$ T-cell count, age, baseline $CD4^+$ T-cell count, and
176 baseline plasma HIV RNA) were screened using Spearman correlation. Among these, 25
177 peptides showed nominal associations with current $CD8^+$ T-cell count at $P < 0.05$ and were
178 selected for subsequent repertoire-level analysis. For each CR, the proportion of these 25
179 CD8-associated peptides recognized (EF>1) was calculated and modeled against current $CD8^+$
180 T-cell count using restricted cubic spline (RCS) regression. The estimated change point was
181 915.5 cells/μL and was rounded to 916 cells/μL for subgroup analyses. CRs were therefore
182 classified as CR ($CD8^+ \geq 916$ cells/μL) (n=10) or CR ($CD8^+ < 916$ cells/μL) (n=28), referred to as
183 CD8-high and CD8-low CRs, respectively. This data-derived classification was specified after
184 exploratory modeling and was considered hypothesis-generating rather than a validated clinical
185 cutoff. Peptide selection and spline estimation used the same participants, so the reported spline
186 P values were exploratory and did not account for the preceding selection step.

187 As a secondary exploratory analysis, 33 HIV-1 peptides differing between CRs and NCs
188 (Benjamini-Hochberg-adjusted $P<0.05$; Figure 2C) were used as a fixed candidate feature set to
189 classify CD8-high (n=10) and CD8-low (n=28) CRs. EF values ≤1 were set to zero, whereas
190 values >1 were log10-transformed. Six classifiers—Gaussian naive Bayes, random forest,
191 XGBoost, elastic-net logistic regression, radial basis function support vector machine, and linear
192 support vector machine—were evaluated using nested cross-validation, with stratified five-fold
193 outer validation repeated 50 times and stratified three-fold inner tuning based on ROC AUC.
194 Within this fixed candidate peptide set, preprocessing, any subsequent feature selection, and
195 hyperparameter optimization were restricted to the training folds. Participant-level out-of-fold

probabilities were averaged across repetitions to generate ROC curves and AUCs, with percentile 95% confidence intervals estimated from 10,000 stratified bootstrap resamples. The candidate peptide set and CD8 threshold had been derived from the full study cohort before cross-validation. Performance estimates were therefore considered exploratory and did not constitute independent validation of a clinical classifier.

External multicenter HIV cohort analysis

To examine whether the longitudinal $CD8^+$ pattern was reproducible on a larger scale, we used data from the multicenter cohort reported by Liu et al., which included 21,862 people with HIV from 31 Chinese provincial-level regions [24]. From this source dataset, we selected 8,178 individuals with $CD4^+$ T-cell counts >500 cells/μL in each of the last three evaluable years. Participants were classified by the last available $CD8^+$ T-cell count as CR ($CD8^+ \geq 916$ cells/μL) (n=3,816) or CR ($CD8^+ < 916$ cells/μL) (n=4,362), and annual $CD8^+$ T-cell measurements were summarized by years since diagnosis. This analysis assessed the reproducibility of longitudinal $CD8^+$ patterns at a larger scale.

HIV-1 Env phylogeny and evolutionary-rate mapping

To explore whether antibody-recognized HIV-1 Env regions differed in evolutionary characteristics, we analyzed 46 publicly available Env gp160 sequences representing major groups, subtypes, and viral strains, with HXB2 used as the coordinate reference. The Env gp160 sequences were aligned using MAFFT version 7 with the --auto strategy, which selected the L-INS-i algorithm [25]. Maximum-likelihood phylogenetic inference was performed using IQ-TREE version 2.4.0, with ModelFinder used for model selection and branch support assessed using 1,000 Shimodaira-Hasegawa-like approximate likelihood ratio test (SH-aLRT) replicates and 1,000 ultrafast bootstrap replicates [26-28]. Site-specific evolutionary rates estimated from the fitted phylogenetic model were mapped to HXB2 coordinates. For each of 177 Env peptides, the median site rate across its mapped HXB2 span was calculated. Peptide-positive rate was

defined as the proportion of CRs with EF>1. Within CR ($CD8^+ \geq 916$ cells/μL) and CR ($CD8^+ < 916$ cells/μL), a peptide was classified as positive when at least one participant had EF>1. An additional peptide-to-strain relationship map summarized whether each HXB2-positioned peptide matched the Env gp160 sequence of a single viral strain or was shared across strain-specific Env sequences from multiple viruses represented in the phylogenetic dataset.

Statistical analysis

Continuous variables are presented as medians (Q1, Q3) and categorical variables as counts (percentages). For the matched NC-CR comparison, continuous clinical variables available in both groups were compared using two-sided exact paired Wilcoxon signed-rank tests; sex was a matching factor and was not tested. Pairwise comparisons of continuous variables among NC, CR ($CD8^+ < 916$ cells/μL), and CR ($CD8^+ \geq 916$ cells/μL) used two-sided Mann-Whitney U tests, and categorical variables were compared using Fisher's exact test or the chi-square test as appropriate. For the six selected clinical variables shown in Figure 4C, between-subgroup effect sizes were estimated using Cliff's δ with 95% confidence intervals; positive values indicated higher values in CD8-high CRs. The corresponding Mann-Whitney U P values were adjusted across the six variables using the Benjamini-Hochberg procedure and reported as q values. Pearson correlation was used for cross-library analyses and Spearman correlation for peptide-clinical and evolutionary-rate analyses. Within each CD8-defined subgroup, median site-rate distributions for antibody-positive and antibody-negative Env peptides were compared using two-sided Mann-Whitney U tests. Peptide-level group comparisons used Benjamini-Hochberg adjustment within the relevant contrast; adjusted $P<0.05$ was considered significant. Longitudinal year-specific subgroup comparisons used two-sided Mann-Whitney U tests and unadjusted P values. All tests were two-sided unless otherwise specified. The

peptide-clinical correlation screen used nominal P values. Associations from this screen and the subsequent data-derived subgroup analyses were interpreted as exploratory.

Use of AI-assisted tools

The authors used Kimi K3.1 Pro (Moonshot AI; used in October 2026) to assist with debugging statistical analysis code and improving the language and clarity of the manuscript. The authors reviewed the AI-assisted code corrections and text revisions and take full responsibility for the accuracy and integrity of the analyses and the final manuscript.

Results

Study cohort and clinical characteristics

The final PhIP-seq cohort included 38 CRs and 38 age- and sex-matched NCs (Figure 1A). All participants were men. Median age was 39.5 years (Q1, Q3: 35.25, 43) in CRs and 40.5 years (35, 46.25) in NCs. CRs had sustained virologic suppression and current $CD4^+$ T-cell counts ≥500 cells/μL. Compared with NCs, CRs showed a higher percentage of $CD8^+$ T cells and a lower CD4/CD8 ratio, although the overall absolute $CD8^+$ T-cell count did not differ significantly (Table 1). CRs also had lower current $CD4^+$ T-cell counts and a lower percentage of $CD4^+$ T cells. When summarized by calendar year, longitudinal $CD4^+$ T-cell counts in CRs increased over follow-up and remained in the immune-reconstituted range during later years (Figure 1B).

Virome-wide antibody profiles differ between CRs and NCs

Virome-wide PhIP-seq showed a broader cumulative antibody signal in CRs than in NCs. Total virscore was higher in CRs (Figure 2B). At the species level, the difference was driven by HIV-1 rather than other viral species. At the peptide level, 34 peptides differed between CRs and NCs after Benjamini-Hochberg correction; 33 were derived from HIV-1 and one from

Epstein-Barr virus (EBV) (Figure 2C). The HIV-1 differences were dominated by Env, with additional signals in other viral proteins (Figure 2D).

Cross-library analysis supported the technical reproducibility of the peptide-level measurements. Across 34 pairs of virus-library peptides and their closest UniRef90 matches, amino-acid sequence identity was strongly associated with cross-library Pearson correlation ($R=0.919$, $P=1.82\times10^{-14}$; Supplementary Figure 1A and Supplementary Table 1). Two representative pairs showed strong sample-level concordance across all 76 participants ($R=0.919$ and $R=0.905$; Supplementary Figure 1B, C).

HIV-1 antibody profiles are associated with current CD8$^+$ T-cell abundance in CRs

PhIP-seq detected antibody reactivity to 571 HIV-derived peptides in at least one participant. These peptides were mapped to their corresponding positions across the HIV-1 genome and encoded proteins, revealing a predominant concentration of antibody reactivity within Env (Figure 3A, B). Among the five clinical variables examined—current CD4$^+$ T-cell count, current CD8$^+$ T-cell count, age, baseline CD4$^+$ T-cell count, and baseline viral load—current CD8$^+$ T-cell count showed the broadest and strongest pattern of nominal associations with peptide EF values. Most of these CD8-associated peptides were derived from HIV-1 Env (Figure 3C).

Among the 571 HIV-derived peptides, 25 showed nominal associations with current CD8$^+$ T-cell count at $P<0.05$ (Figure 3C). The proportion of these 25 CD8-associated peptides recognized by each CR ($EF>1$) was analyzed using restricted cubic spline (RCS) regression, which demonstrated a nonlinear association with current CD8$^+$ T-cell count (overall $P=0.0048$; P for nonlinearity=0.0027). The fitted curve yielded an estimated change point of 915.5 cells/μL (Figure 3D). We therefore used 916 cells/μL as an exploratory threshold. Among the 38 CRs, 10 were assigned to the CR (CD8$^+\geq$916 cells/μL) subgroup and 28 to the CR (CD8$^+<$916 cells/μL) subgroup. Exploratory classification models using the 33 HIV-1 peptides that differed between CRs and NCs were used to distinguish CD8-high from CD8-low CRs. Among the six classifiers

evaluated using repeated nested cross-validation, Gaussian naive Bayes yielded the highest area under the receiver operating characteristic curve (AUC=0.739; Figure 3E), indicating modest discrimination.

High-CD8 CRs show persistent longitudinal CD8$^+$ T-cell elevation

The two CD8-defined subgroups were similar in age, age at HIV diagnosis, ART duration, and baseline HIV RNA (Table 2). A clear divergence emerged in CD8-related measures: CR (CD8$^+$<916 cells/μL) had absolute CD8$^+$ T-cell counts similar to those in NCs, whereas CR (CD8$^+$≥916 cells/μL) showed markedly elevated absolute CD8$^+$ T-cell counts and percentages. Direct comparison of the CR subgroups confirmed higher CD8$^+$ T-cell counts in the high-CD8 subgroup [1198 vs. 627.5 cells/μL; P<0.0001] and a lower CD4/CD8 ratio in CR (CD8$^+$≥916 cells/μL) [0.72 (0.59, 0.87) vs. 1.36 (1.09, 1.54); P=0.0002]. Current CD4$^+$ T-cell counts were similar between the CR subgroups [790 (712, 898.75) vs. 720.5 (645, 907.25) cells/μL; P=0.2018], whereas baseline CD4$^+$ T-cell counts were lower in CR (CD8$^+$≥916 cells/μL) [251.5 (187.5, 413.25) vs. 437 (358, 518) cells/μL; P=0.0088]. The interval from HIV diagnosis to virologic suppression was also shorter in CR (CD8$^+$≥916 cells/μL) [172.5 (167.25, 177.5) vs. 187.5 (175.5, 397.25) days; P=0.0129]. Effect-size analysis confirmed lower baseline CD4$^+$ T-cell counts (Cliff's δ=−0.57) and a shorter interval to virologic suppression (Cliff's δ=−0.54) in the high-CD8 subgroup; both comparisons remained significant after Benjamini-Hochberg adjustment (q=0.0387; Figure 4C), whereas current CD4$^+$ T-cell count, baseline viral load, age, and time on ART did not differ significantly after adjustment.

Longitudinal analysis showed that the CD8$^+$ difference was not confined to the sampling visit. CD8$^+$ T-cell counts in CR (CD8$^+$≥916 cells/μL) were already higher at the earliest evaluable follow-up and remained higher through years 1-10, whereas CD4$^+$ T-cell differences were concentrated at the earliest time point and subsequently converged (Figure 4A, B). Thus, the

dominant longitudinal distinction between the two CR phenotypes was a stable $CD8^+$ trajectory rather than persistent separation of $CD4^+$ T-cell counts.

The longitudinal $CD8^+$ pattern was reproduced in the external multicenter cohort. Among 8,178 candidate immune-reconstituted participants, 3,816 were classified as CR ($CD8^+ \geq 916$ cells/μL) and 4,362 as CR ($CD8^+ < 916$ cells/μL) by the last available $CD8^+$ T-cell count. The two groups remained clearly separated in $CD8^+$ T-cell counts across follow-up years (Supplementary Figure 2).

High-CD8 CRs have a broader antiviral antibody signature

Both CD8-defined CR subgroups differed from NCs in their antibody profiles, with more extensive differences in the comparison between CR ($CD8^+ \geq 916$ cells/μL) and NCs. Most differential peptides were derived from HIV-1, with additional signals from non-HIV viruses, including CMV, EBV, pseudocowpox virus (PCPV), herpes simplex virus types 1 and 2 (HSV-1 and HSV-2), macacine alphaherpesvirus 1 (McAHV-1), salivirus A (SalV-A), and salivirus FHB (SalV-FHB) (Figure 5A). The corresponding peptide EF distributions further showed that these differences involved multiple HIV-1 gp41 peptides, other HIV-1 peptides, and peptides derived from non-HIV viruses (Supplementary Figure 3A-C).

The overlap and unique components of the peptide-comparison sets are summarized in Figure 5B. The CR ($CD8^+ \geq 916$ cells/μL)-versus-NC comparison identified 74 differential peptides, comprising 54 HIV-1 and 20 non-HIV peptides. This set contained all 34 peptides identified in the overall CR-versus-NC comparison. Of these 34 peptides, 30 were also identified in the CR ($CD8^+ < 916$ cells/μL)-versus-NC comparison. In addition, 40 peptides were uniquely identified in the CR ($CD8^+ \geq 916$ cells/μL)-versus-NC comparison, including 21 HIV-1 peptides and 19 non-HIV peptides from CMV, EBV, HSV-1, HSV-2, PCPV, McAHV-1, SalV-A, and SalV-FHB.

At the HIV-1 protein level, both CD8-defined CR subgroups had more antibody-reactive peptides relative to NCs in Env, Gag-Pol, Rev, Gag, and Vpu (Figure 5C). Total virscore was also significantly higher in CR ($CD8^+ \geq 916$ cells/μL) than in NCs, whereas no significant difference was observed between CR ($CD8^+ < 916$ cells/μL) and NCs (Figure 5D). Together, these findings indicate that the broader antiviral antibody signature was concentrated predominantly in CR ($CD8^+ \geq 916$ cells/μL).

Env peptide recognition differs in relation to evolutionary rate

To explore whether HIV-1 Env antibody recognition preferentially targets regions with different evolutionary characteristics, we identified 177 Env gp160 peptides that were recognized by antibodies in at least one participant, mapped them to prototypic HXB2 coordinates, and constructed a maximum-likelihood phylogeny from 46 publicly available Env gp160 sequences (Figure 6A and Supplementary Figure 4). Mapping the 177 HXB2-positioned peptides back to the strain-specific Env sequences used for phylogenetic analysis showed that 157 peptides (88.7%) matched only one Env sequence, whereas 20 (11.3%) were shared across Env sequences from 2-7 viral strains (Supplementary Figure 5). Across all 177 peptides, the peptide-positive rate among CRs showed a weak positive correlation with median IQ-TREE site evolutionary rate (Spearman $\rho=0.182$, $P=0.016$; Figure 6B), suggesting that HIV-1 Env antibody recognition frequency was not strongly associated with local evolutionary rate and was therefore unlikely to be a major determinant of the observed evolutionary-rate differences among recognized peptides.

Within CR ($CD8^+ \geq 916$ cells/μL), 81 peptides were positive in at least one participant and 96 were negative; their evolutionary-rate distributions did not differ significantly ($P=0.750$). Within CR ($CD8^+ < 916$ cells/μL), 93 peptides were positive and 84 were negative, and positive peptides had higher median site rates than negative peptides ($P=7.40\times10^{-5}$; Figure 6C).

Discussion

In this study, we used virome-wide antibody profiling to examine an immune-reconstituted population that has received relatively limited attention. Most studies of immune reconstitution in treated HIV infection have focused on immunological non-responders and the mechanisms underlying inadequate $CD4^+$ T-cell recovery, whereas individuals with successful $CD4^+$ T-cell recovery have commonly served as reference populations [2,3]. Consequently, CRs are often considered to represent a relatively favorable, homogeneous state of immune recovery. However, recovery of $CD4^+$ T-cell counts does not necessarily indicate complete immune reconstitution. Previous studies have shown that even among individuals with sustained viral suppression and $CD4^+$ T-cell counts ≥500 cells/μL, persistent $CD8^+$ T-cell expansion, low CD4/CD8 ratios, immune activation, senescence, and inflammatory abnormalities may remain [7-10,29]. Using virome-wide antibody profiling, we identified two immunologically distinct subgroups within CRs despite similar current $CD4^+$ T-cell counts. These subgroups differed not only in their antiviral antibody profiles but also in $CD8^+$ T-cell counts. Notably, the difference in $CD8^+$ T-cell counts persisted during long-term follow-up.

Virome-wide antibody profiling revealed an additional dimension of this heterogeneity. Although PhIP-seq and related VirScan approaches can interrogate thousands of viral peptides simultaneously, the systematic application of virome-wide antibody repertoire profiling remains limited in people with HIV. Previous studies have mainly characterized HIV-specific antibody evolution, compared antibody profiles between spontaneous and treatment-induced viral control, or identified HIV antibody targets associated with viral load and viremic control [13-16]. In our study, the overall CR-versus-NC comparison identified 34 differential peptides, including 33 HIV-1 peptides predominantly mapping to Env. More importantly, $CD8^+$ T-cell stratification revealed a substantially wider range of differences: CR ($CD8^+$≥916 cells/μL) showed 74 differential peptides versus NCs, including all 34 peptides from the overall comparison together with 40 newly identified HIV and non-HIV peptides, whereas the differences between CR

(CD8$^+$<916 cells/μL) and NCs were considerably less extensive. These findings extend previous observations of persistent cellular abnormalities after CD4$^+$ T-cell recovery to the antiviral antibody repertoire and indicate that conventional CD4$^+$ T-cell recovery does not define a uniform state of immune reconstitution.

The broader non-HIV antibody recognition in CR (CD8$^+$≥916 cells/μL) may reflect a greater cumulative history of viral antigen exposure rather than ongoing viral replication at the time of sampling. Several of the additional peptides were derived from herpesviruses, including CMV, EBV, and HSV-1/2, which establish lifelong latency and may undergo intermittent reactivation. In the setting of HIV infection, repeated or subclinical reactivation of these viruses could periodically boost virus-specific humoral responses, leaving durable antibody signatures even after CD4$^+$ T-cell recovery. Such recurrent antigenic stimulation may also contribute to long-term expansion of virus-specific effector and memory CD8$^+$ T cells. CMV provides a well-established example: CMV coinfection has been linked to CD8$^+$ T-cell expansion and inflammation during suppressive ART, while stronger CMV-directed humoral responses have been associated with poorer CD4$^+$ T-cell recovery and greater T-cell activation [18,19]. Pharmacologic suppression of CMV can reduce T-cell activation, and subclinical CMV replication during early HIV infection has been associated with a lower subsequent CD4/CD8 ratio [30,31]. Notably, baseline CD4$^+$ T-cell count emerged as a principal clinical factor associated with the persistent high-CD8 phenotype. Among the clinical variables examined, it showed one of the largest between-group effect sizes and remained significant after adjustment for multiple comparisons. CD8-high CRs had substantially lower baseline CD4$^+$ T-cell counts despite similar sampling-time CD4$^+$ T-cell counts, highlighting the potential importance of the severity of pre-ART immunodeficiency, rather than the degree of current CD4$^+$ T-cell recovery, in shaping the subsequent immune phenotype. More profound pre-ART CD4$^+$ T-cell depletion may have increased opportunities for latent-virus reactivation or broader antigenic stimulation

before immune recovery. Thus, the broader non-HIV antibody repertoire and persistent $CD8^+$ T-cell expansion may represent complementary humoral and cellular footprints of cumulative antiviral immune stimulation rooted, at least in part, in more severe baseline immune damage.

A similar interpretation may also apply to HIV-specific antibody recognition. HIV-1 Env accounted for most of the peptide-level differences, and broader HIV-specific antibody responses have previously been associated with greater or more prolonged antigen exposure, higher viral burden, and greater Env diversity [13-16,32-34]. Although PhIP-seq measures recognition of linear peptides rather than neutralization breadth, the broader HIV peptide recognition observed in CR ($CD8^+ \geq 916$ cells/μL) may likewise reflect a more extensive history of HIV antigenic stimulation before effective viral suppression.

Given the strong immune selection acting on HIV-1 Env [35], we further examined whether antibody recognition was related to local evolutionary rate. Across 177 mapped Env peptides, the peptide-positive rate was only weakly associated with median site evolutionary rate. However, subgroup patterns differed: in CR ($CD8^+ < 916$ cells/μL), antibody-positive peptides mapped to regions with higher evolutionary rates than antibody-negative peptides, whereas this difference was absent in CR ($CD8^+ \geq 916$ cells/μL). One possible explanation is that greater cumulative HIV antigenic stimulation in the persistent high-CD8 subgroup generated broader and more durable antibody memory while repeated immune selection and viral escape progressively reshaped Env sequences, weakening the correspondence between retained antibody recognition and local evolutionary rate. The lower baseline $CD4^+$ T-cell counts in this subgroup are compatible with such a history. These findings remain exploratory and require validation using longitudinal autologous Env sequences and functional antibody assays.

Although our study provides new insights into immune heterogeneity among CRs, particularly by revealing distinct antibody repertoires associated with persistent differences in the $CD8^+$ T-cell compartment, several limitations should be acknowledged. First, the PhIP-seq cohort was

relatively small, and CR ($CD8^+ \geq 916$ cells/μL) included only 10 participants. All participants were men from a single center, which limits generalizability, although this male predominance is consistent with the epidemiologic profile of treated people with HIV in Beijing [36]. Second, the 916 cells/μL threshold and peptide-based classifier were derived and evaluated in the same cohort and should therefore be considered exploratory. Third, PhIP-seq does not assess conformational epitopes, antibody concentrations, neutralizing activity, B-cell clonality, tissue-specific responses, or active viral replication, and sequence homology among related viruses may contribute to cross-reactive signals [37].

Conclusions

Our study provides novel evidence that CRs with comparable $CD4^+$ T-cell recovery remain immunologically heterogeneous, with virome-wide antibody profiling revealing distinct antibody repertoires and persistent differences in $CD8^+$ T-cell counts. Persistent $CD8^+$ T-cell elevation was associated with broader HIV and non-HIV antibody recognition and distinct Env evolutionary patterns, suggesting residual immune perturbation beyond conventional $CD4^+$ T-cell recovery. These findings highlight the clinical relevance of $CD8^+$ T-cell dynamics in assessing immune reconstitution and suggest that CRs with persistently elevated $CD8^+$ T-cell counts may warrant continued immunologic surveillance even after sustained virologic suppression and $CD4^+$ T-cell recovery.

List of abbreviations

ART, antiretroviral therapy; AUC, area under the receiver operating characteristic curve; CI, confidence interval; CMV, cytomegalovirus; CR, complete immune-reconstitution responder; EBV, Epstein-Barr virus; EF, enrichment factor; Env, envelope; HIV, human immunodeficiency virus; HSV, herpes simplex virus; INR, immunological non-responder; McAHV-1, macacine alphaherpesvirus 1; NC, HIV-negative control; NR, normalized read count; PCPV, pseudocowpox virus; PhIP-seq, phage immunoprecipitation sequencing; Q1, first quartile; Q3,

third quartile; RCS, restricted cubic spline; ROC, receiver operating characteristic; SalV-A, salivirus A; SalV-FHB, salivirus FHB; SH-aLRT, Shimodaira-Hasegawa-like approximate likelihood ratio test.

Declarations

Ethics approval and consent to participate

The study was conducted in accordance with the Declaration of Helsinki and approved by the Institutional Ethics Committee of Beijing Ditan Hospital, Capital Medical University (No. DTEC-KY2024-006-02; February 2, 2024). Written informed consent was obtained from all participants before sample collection.

Consent for publication

Not applicable.

Availability of data and materials

Deidentified participant-level data supporting this study may be made available from the corresponding author upon reasonable request, subject to participant consent, institutional approval, and applicable privacy protections. Analytic code may be shared under the same conditions. The public multicenter cohort data were obtained from the repository accompanying Liu et al. [24].

Competing interests

The authors declare that they have no competing interests.

Funding

This work was supported by the Capital's Funds for Health Improvement and Research, Key Research Program (No. 2024-1-1203); the Beijing Municipal Health Commission High-Level Public Health Technical Talent Development Program, Discipline Leader track (No. Discipline Leader-3-21); and the Beijing Hospitals Authority Dengfeng Talent Support Program (No. DFL20221601).

Authors' contributions

XL, XZ, and GL designed and supervised the research. XL was the principal investigator. Hui L, CS, Huan L, DC, RQ, SZ, YG, and YD collected clinical data and samples. ZZ and GL performed PhIP-seq and data analyses and drafted the manuscript. XL and XZ revised the manuscript. All authors contributed to the manuscript and approved the final version. Hui L denotes Hui Liu; Huan L denotes Huan Liu.

Acknowledgements

The authors thank all study participants and the clinical and laboratory staff who contributed to sample collection, longitudinal data management, and PhIP-seq experiments.

References

1. INSIGHT START Study Group. Initiation of antiretroviral therapy in early asymptomatic HIV infection. N Engl J Med. 2015;373:795-807. doi: 10.1056/NEJMoa1506816.

2. Xiao Q, Yan L, Han J, Yang S, Tang Y, Li Q, et al. Metabolism-dependent ferroptosis promotes mitochondrial dysfunction and inflammation in $CD4^+$ T lymphocytes in HIV-infected immune non-responders. EBioMedicine. 2022;86:104382. doi: 10.1016/j.ebiom.2022.104382.

3. Liu X, Zhang L, Li X, Chen L, Lu L, Yang Y, et al. Single-cell multi-omics profiling uncovers the immune heterogeneity in HIV-infected immunological non-responders. EBioMedicine. 2025;115:105667. doi: 10.1016/j.ebiom.2025.105667.

4. Geng Y, Jia H, Guan Y, Ren R, Zhao D, Gan X, et al. Five-Year Immune Recovery After ART Initiation Among PLWH Aged ≥15 Years with Baseline Immunosuppression—China, 2013-2024. China CDC Wkly. 2026;8:772-779. doi: 10.46234/ccdcw2026.125.

5. Liu J, Wang L, Hou Y, Zhao Y, Dou Z, Ma Y, et al. Immune restoration in HIV-1-infected patients after 12 years of antiretroviral therapy: a real-world observational study. Emerg Microbes Infect. 2020;9:2550-2561. doi: 10.1080/22221751.2020.1840928.

6. Handoko R, Colby DJ, Kroon E, Sacdalan C, de Souza M, Pinyakorn S, et al. Determinants of suboptimal CD4+ T cell recovery after antiretroviral therapy initiation in a prospective cohort of acute HIV-1 infection. J Int AIDS Soc. 2020;23:e25585. doi: 10.1002/jia2.25585.

7. Shu Y, Zhang M, Li J, Deng X, Liu J, Yang C, et al. Trajectories of CD4 T-cell count, CD8 T-cell count, and CD4/CD8 ratio in patients with HIV and long-term virological suppression based on Yunnan HIV cohort. HIV Med. 2025;26:70-80. doi: 10.1111/hiv.13707.

8. Hu Y, Ge L, He Y, Li X, Luo Y, Wu H, et al. Persistent CD8+ T cell-driven immune dysregulation despite normalized CD4+ T cell recovery in ART-treated people living with HIV. Front Immunol. 2026;17:1735779. doi: 10.3389/fimmu.2026.1735779.

526 9. Trickey A, May MT, Schommers P, Tate J, Ingle SM, Guest JL, et al. CD4:CD8 ratio and
527 CD8 count as prognostic markers for mortality in human immunodeficiency virus-infected
528 patients on antiretroviral therapy: the Antiretroviral Therapy Cohort Collaboration (ART-CC).
529 Clin Infect Dis. 2017;65:959-966. doi: 10.1093/cid/cix466.

530 10. Deeks SG, Tracy R, Douek DC. Systemic effects of inflammation on health during chronic
531 HIV infection. Immunity. 2013;39:633-645. doi: 10.1016/j.immuni.2013.10.001.

532 11. Xu GJ, Kula T, Xu Q, Li MZ, Vernon SD, Ndung'u T, et al. Viral immunology.
533 Comprehensive serological profiling of human populations using a synthetic human virome.
534 Science. 2015;348:aaa0698. doi: 10.1126/science.aaa0698.

535 12. Mohan D, Wansley DL, Sie BM, Noon MS, Baer AN, Laserson U, et al. PhIP-Seq
536 characterization of serum antibodies using oligonucleotide-encoded peptidomes. Nat Protoc.
537 2018;13:1958-1978. doi: 10.1038/s41596-018-0025-6.

538 13. Eshleman SH, Laeyendecker O, Kammers K, Chen A, Sivay MV, Kottapalli S, et al.
539 Comprehensive profiling of HIV antibody evolution. Cell Rep. 2019;27:1422-1433.e4. doi:
540 10.1016/j.celrep.2019.03.097.

541 14. Kammers K, Chen A, Monaco DR, Hudelson SE, Grant-McAuley W, Moore RD, et al. HIV
542 antibody profiles in HIV controllers and persons with treatment-induced viral suppression. Front
543 Immunol. 2021;12:740395. doi: 10.3389/fimmu.2021.740395.

544 15. Grant-McAuley W, Morgenlander W, Hudelson SE, Thakar M, Piwowar-Manning E, Clarke
545 W, et al. Comprehensive profiling of pre-infection antibodies identifies HIV targets associated
546 with viremic control and viral load. Front Immunol. 2023;14:1178520. doi:
547 10.3389/fimmu.2023.1178520.

548 16. Grant-McAuley W, Morgenlander WR, Ruczinski I, Kammers K, Laeyendecker O,
549 Hudelson SE, et al. Identification of antibody targets associated with lower HIV viral load and
550 viremic control. PLoS One. 2024;19:e0305976. doi: 10.1371/journal.pone.0305976.

551 17. Song W, Craft J. T follicular helper cell heterogeneity. Annu Rev Immunol.
552 2024;42:127-152. doi: 10.1146/annurev-immunol-090222-102834.

553 18. Freeman ML, Mudd JC, Shive CL, Younes SA, Panigrahi S, Sieg SF, et al. CD8 T-cell
554 expansion and inflammation linked to CMV coinfection in ART-treated HIV infection. Clin
555 Infect Dis. 2016;62:392-396. doi: 10.1093/cid/civ840.

556 19. Gómez-Mora E, Massanella M, García E, Giles D, Bernadó M, Urrea V, et al. Elevated
557 humoral response to cytomegalovirus in HIV-infected individuals with poor $CD4^+$ T-cell
558 immune recovery. PLoS One. 2017;12:e0184433. doi: 10.1371/journal.pone.0184433.

559 20. Chen S, Zhou Y, Chen Y, Gu J. fastp: an ultra-fast all-in-one FASTQ preprocessor.
560 Bioinformatics. 2018;34:i884-i890. doi: 10.1093/bioinformatics/bty560.

561 21. Martin M. Cutadapt removes adapter sequences from high-throughput sequencing reads.
562 EMBnet J. 2011;17:10-12. doi: 10.14806/ej.17.1.200.

563 22. Shen W, Le S, Li Y, Hu F. SeqKit: a cross-platform and ultrafast toolkit for FASTA/Q file
564 manipulation. PLoS One. 2016;11:e0163962. doi: 10.1371/journal.pone.0163962.

565 23. Li H, Durbin R. Fast and accurate short read alignment with Burrows-Wheeler transform.
566 Bioinformatics. 2009;25:1754-1760. doi: 10.1093/bioinformatics/btp324.

567 24. Liu F, Zhang H, Wang X, Huang J, Shi J, Yang Z, et al. Dynamic prediction of HIV-related
568 incomplete immune reconstitution: A multicenter, large cohort study using advanced joint
569 modeling. Sci Adv. 2026;12:eaeb2781. doi: 10.1126/sciadv.aeb2781.

570 25. Katoh K, Standley DM. MAFFT multiple sequence alignment software version 7:
571 improvements in performance and usability. Mol Biol Evol. 2013;30:772-780. doi:
572 10.1093/molbev/mst010.

573 26. Minh BQ, Schmidt HA, Chernomor O, Schrempf D, Woodhams MD, von Haeseler A, et al.
574 IQ-TREE 2: new models and efficient methods for phylogenetic inference in the genomic era.
575 Mol Biol Evol. 2020;37:1530-1534. doi: 10.1093/molbev/msaa015.

576 27. Kalyaanamoorthy S, Minh BQ, Wong TKF, von Haeseler A, Jermiin LS. ModelFinder: fast
577 model selection for accurate phylogenetic estimates. Nat Methods. 2017;14:587-589. doi:
578 10.1038/nmeth.4285.

579 28. Hoang DT, Chernomor O, von Haeseler A, Minh BQ, Vinh LS. UFBoot2: improving the
580 ultrafast bootstrap approximation. Mol Biol Evol. 2018;35:518-522. doi:
581 10.1093/molbev/msx281.

582 29. Garrido-Rodríguez V, Bulnes-Ramos Á, Olivas-Martínez I, Pozo-Balado MDM,
583 Álvarez-Ríos AI, Gutiérrez F, et al. The persistence of low CD4/CD8 ratio in chronic
584 HIV-infection, despite ART suppression and normal CD4 levels, is associated with pre-therapy
585 values of inflammation and thymic function. J Microbiol Immunol Infect. 2024;57:854-867. doi:
586 10.1016/j.jmii.2024.08.007.

587 30. Hunt PW, Martin JN, Sinclair E, Epling L, Teague J, Jacobson MA, et al. Valganciclovir
588 reduces T cell activation in HIV-infected individuals with incomplete CD4+ T cell recovery on
589 antiretroviral therapy. J Infect Dis. 2011;203:1474-1483. doi: 10.1093/infdis/jir060.

590 31. Smith DM, Nakazawa M, Freeman ML, Anderson CM, Oliveira MF, Little SJ, et al.
591 Asymptomatic CMV replication during early human immunodeficiency virus (HIV) infection is
592 associated with lower CD4/CD8 ratio during HIV treatment. Clin Infect Dis.
593 2016;63:1517-1524. doi: 10.1093/cid/ciw612.

32. Piantadosi A, Panteleeff D, Blish CA, Baeten JM, Jaoko W, McClelland RS, et al. Breadth of neutralizing antibody response to human immunodeficiency virus type 1 is affected by factors early in infection but does not influence disease progression. J Virol. 2009;83:10269-10274. doi: 10.1128/JVI.01149-09.

33. Gray ES, Madiga MC, Hermanus T, Moore PL, Wibmer CK, Tumba NL, et al. The neutralization breadth of HIV-1 develops incrementally over four years and is associated with CD4+ T cell decline and high viral load during acute infection. J Virol. 2011;85:4828-4840. doi: 10.1128/JVI.00198-11.

34. Whitehill GD, Joy J, Marino FE, Krause R, Mallick S, Courtney H, et al. Autologous neutralizing antibody responses after antiretroviral therapy in acute and early HIV-1. J Clin Invest. 2024;134:e176673. doi: 10.1172/JCI176673.

35. Frost SDW, Wrin T, Smith DM, Kosakovsky Pond SL, Liu Y, Paxinos E, et al. Neutralizing antibody responses drive the evolution of human immunodeficiency virus type 1 envelope during recent HIV infection. Proc Natl Acad Sci U S A. 2005;102:18514-18519. doi: 10.1073/pnas.0504658102.

36. Zhang J, Zhou M, Wang P, Wang D, Mi Y, Liu J, et al. Temporal trends of clinical characteristics and treatments in people living with HIV at the initiation of antiretroviral therapy—Beijing Municipality, China, 2010-2020. China CDC Wkly. 2023;5:131-136. doi: 10.46234/ccdcw2023.024.

37. Monaco DR, Kottapalli SV, Breitwieser FP, Anderson DE, Wijaya L, Tan K, et al. Deconvoluting virome-wide antibody epitope reactivity profiles. EBioMedicine. 2022;75:103747. doi: 10.1016/j.ebiom.2021.103747.

Figure

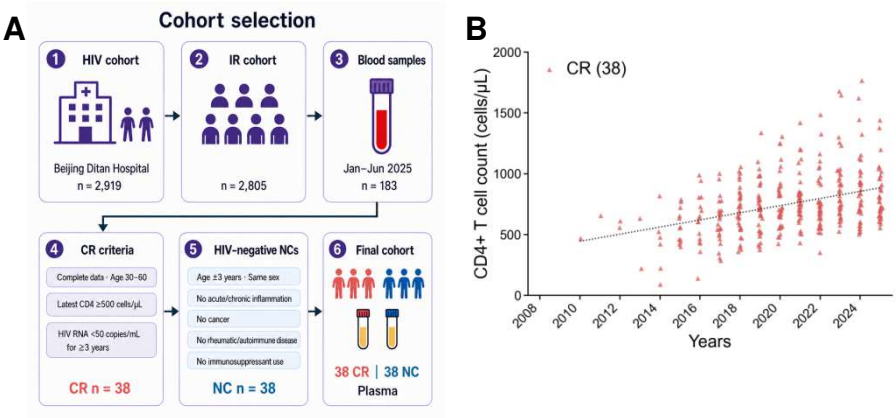

Figure 1: Study cohort and longitudinal CD4⁺ T-cell recovery. (A) Participant-selection workflow from the source HIV cohort (n=2,919) to the final PhIP-seq cohort of 38 CRs and 38 age- and sex-matched NCs; CR eligibility and NC exclusion criteria are summarized in the flowchart. (B) Individual longitudinal CD4⁺ T-cell measurements in CRs from 2008 to 2025 with the fitted overall trajectory. CR: complete immune-reconstitution responder; NC: HIV-negative control.

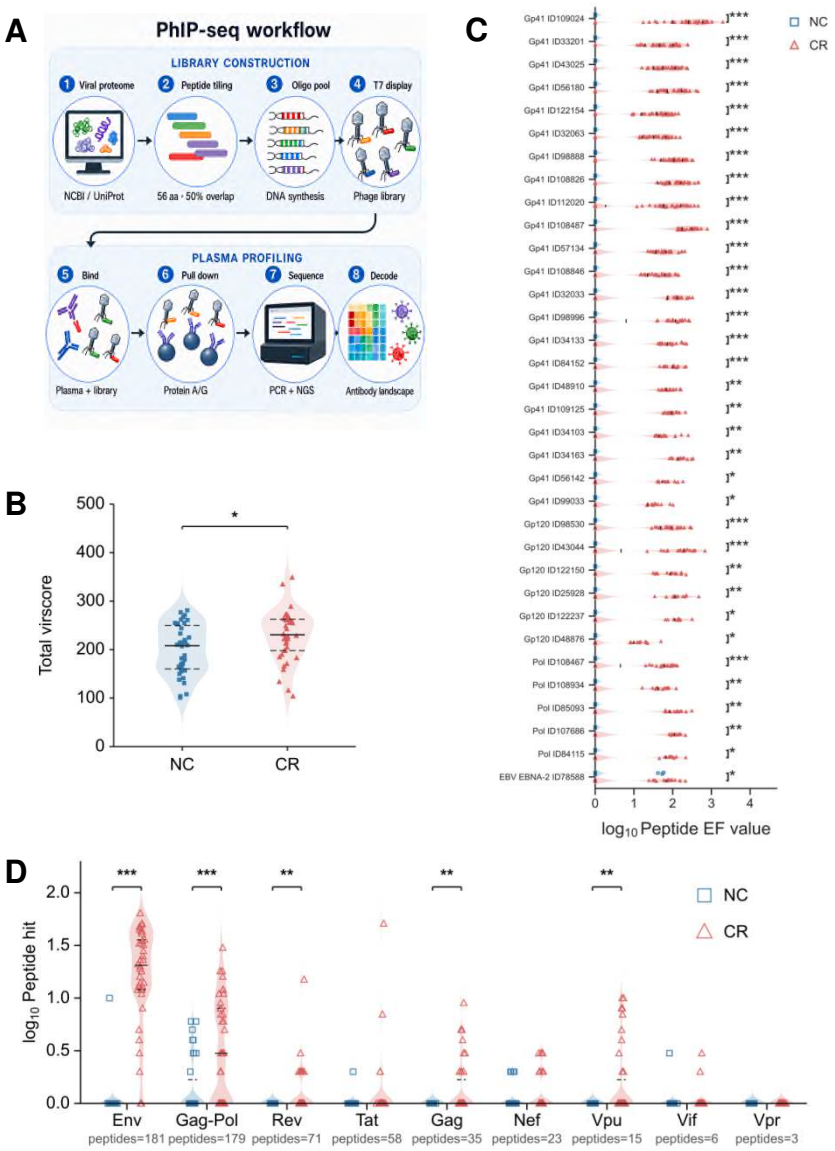

Figure 2: Virome-wide antibody profiling in CRs and NCs. (A) T7 PhIP-seq library construction, plasma immunoprecipitation, sequencing, and antibody-profile analysis workflow. (B) Total virscore distributions in NCs and CRs. (C) Participant-level EF values for the 34 peptides that differed between CRs and NCs after Benjamini-Hochberg adjustment. (D) HIV-1 protein-level peptide-hit distributions across Env, Gag-Pol, Rev, Tat, Gag, Nef, Vpu, Vif, and Vpr. EF: enrichment factor. *P<0.05, **P<0.01, and ***P<0.001.

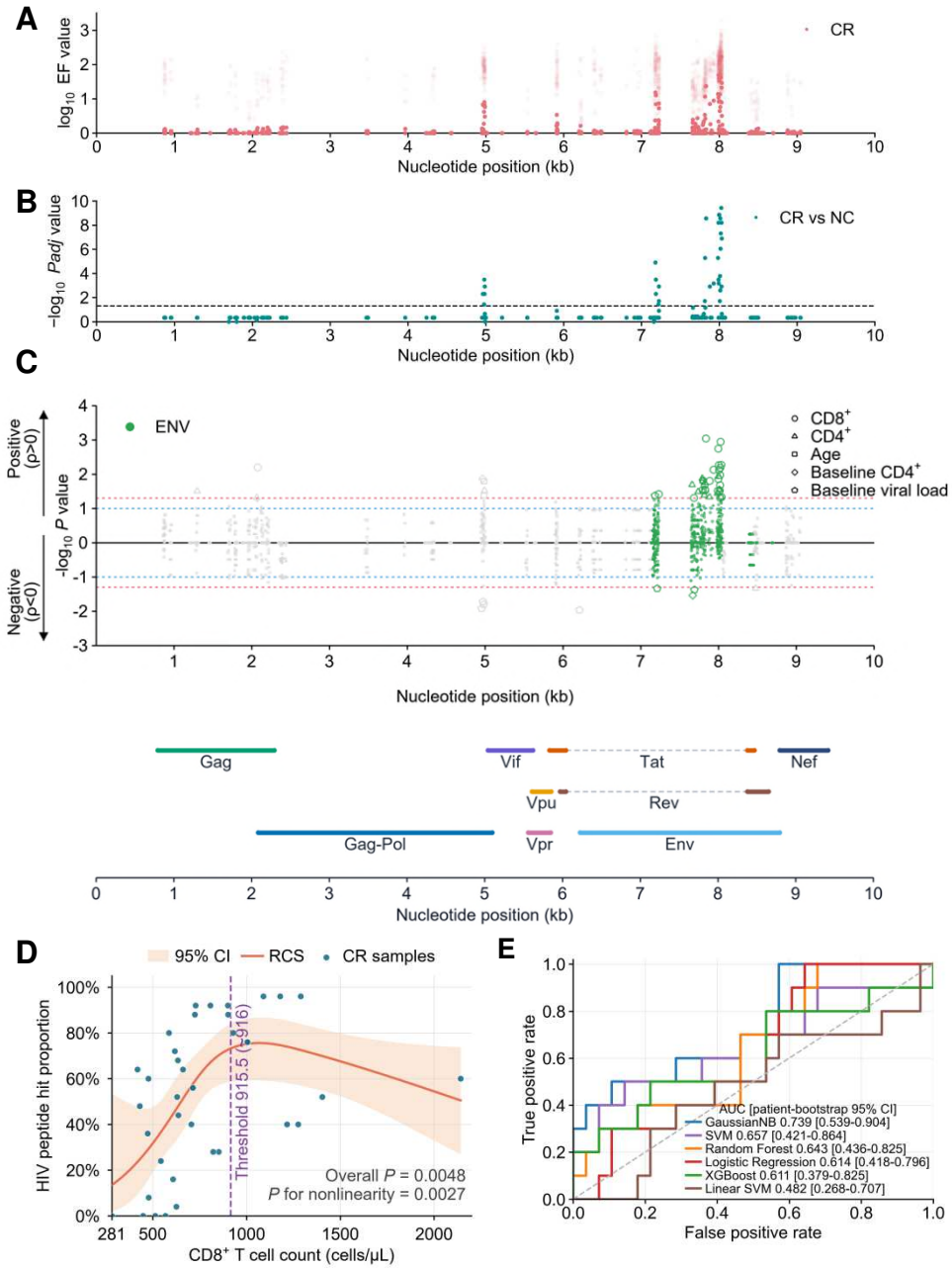

Figure 3: HIV-1 peptide reactivity and its association with CD8⁺ T-cell abundance in CRs. (A) Genome-wide distribution of EF values for HIV-derived peptides reactive in CRs. (B) Genomic positions and adjusted *P* values of HIV-1 peptides differing between CRs and NCs. (C) Direction and significance of Spearman associations between peptide EF values and current CD8⁺ T-cell count, current CD4⁺ T-cell count, age, baseline CD4⁺ T-cell count, and baseline HIV RNA; Env-derived peptides are highlighted. (D) Restricted cubic spline relating current CD8⁺ T-cell count to the proportion of 25 CD8-associated peptides recognized (EF>1); the shaded area indicates the 95% confidence interval and the vertical dashed line marks the estimated change point at 915.5 cells/μL. (E) Cross-validated receiver operating characteristic curves for six exploratory classifiers using the 33 CR-versus-NC differential HIV-1 peptides to distinguish CR (CD8⁺≥916 cells/μL) from CR (CD8⁺<916 cells/μL). EF: enrichment factor.

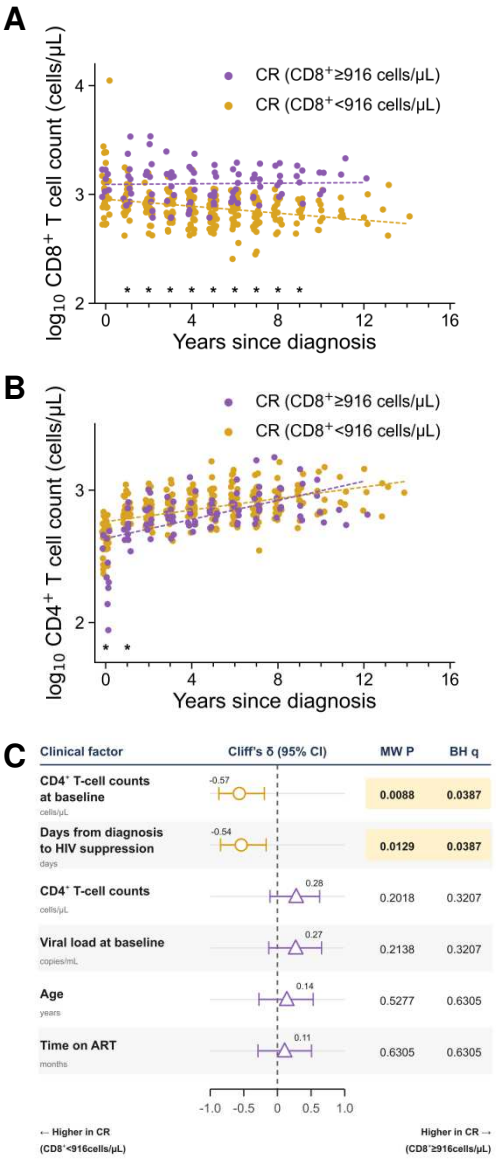

Figure 4: Longitudinal T-cell trajectories and selected clinical characteristics in CD8-defined CR subgroups. Individual annual measurements are shown by years since HIV diagnosis for CR (CD8⁺≥916 cells/μL; n=10) and CR (CD8⁺<916 cells/μL; n=28), with fitted subgroup trajectories. (A) Log10-transformed CD8⁺ T-cell counts. (B) Log10-transformed CD4⁺ T-cell counts. Year-specific between-group comparisons in (A) and (B) used two-sided Mann-Whitney U tests. **P*<0.05 (unadjusted). (C) Cliff's δ effect sizes and 95% confidence intervals for selected clinical variables. Negative values indicate higher values in CR (CD8⁺<916 cells/μL), whereas positive values indicate higher values in CR (CD8⁺≥916 cells/μL). MW *P* values were obtained using two-sided Mann-Whitney U tests, and BH *q* values were calculated using the Benjamini-Hochberg procedure. ART: antiretroviral therapy.

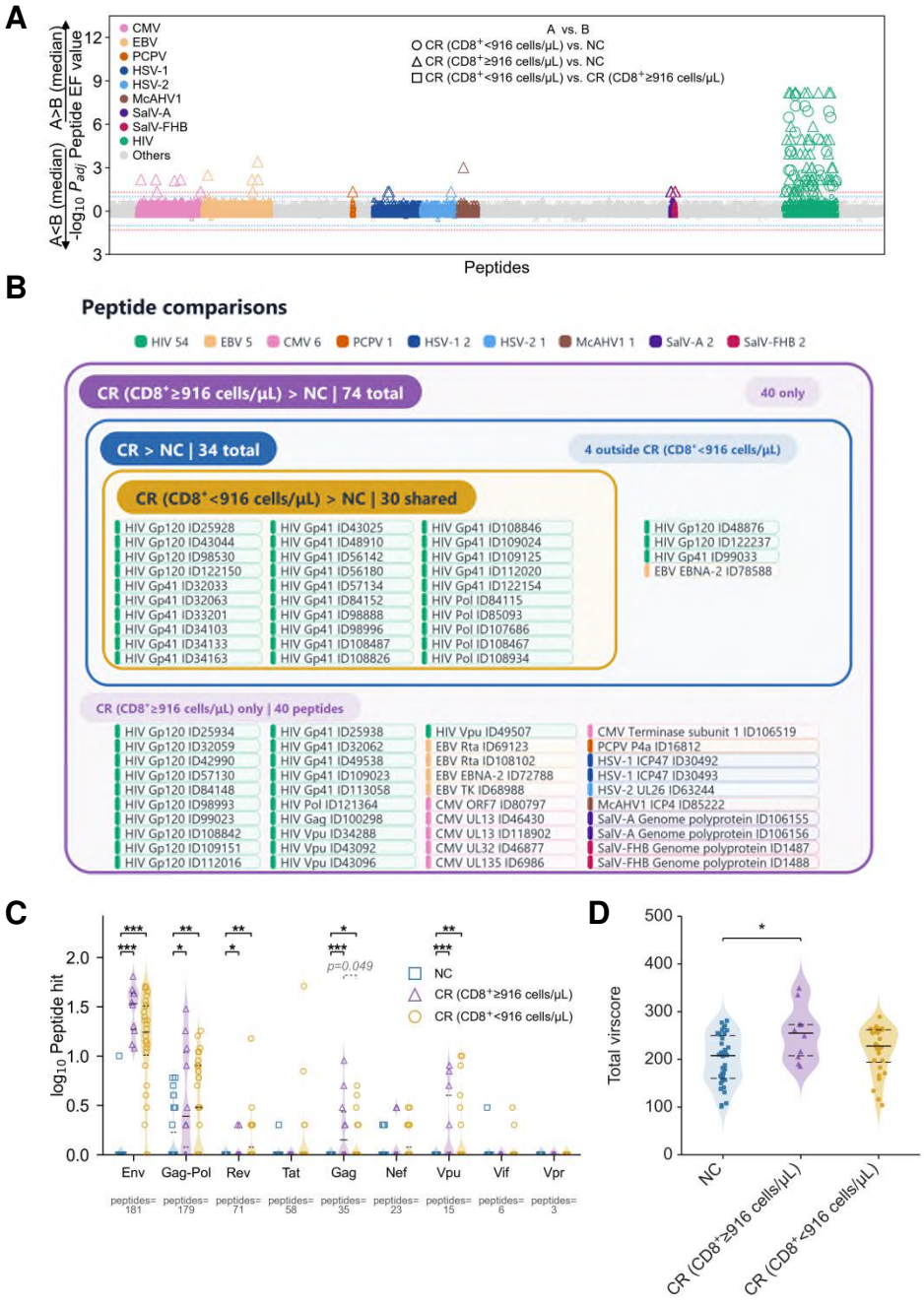

Figure 5: Virome-wide antibody signatures according to CD8⁺ T-cell status in CRs. (A) Directional peptide-level differential-significance plot for pairwise comparisons among NCs, CR (CD8⁺≥916 cells/μL), and CR (CD8⁺<916 cells/μL); colors indicate viral origin and symbols indicate the comparison. (B) Schematic summary of overlap among the overall CR-versus-NC and CD8-subgroup-versus-NC differential-peptide sets. The 74 peptides identified in CR (CD8⁺≥916 cells/μL) versus NCs contained all 34 overall CR-versus-NC peptides; 30 of the 34 were also identified in CR (CD8⁺<916 cells/μL) versus NCs, and 40 additional peptides were identified only in the high-CD8 comparison. (C) HIV-1 protein-level peptide-hit distributions across Env, Gag-Pol, Rev, Tat, Gag, Nef, Vpu, Vif, and Vpr in the three groups. (D) Total virscore distributions in the three groups. *P<0.05, **P<0.01, ***P<0.001, and ****P<0.0001.

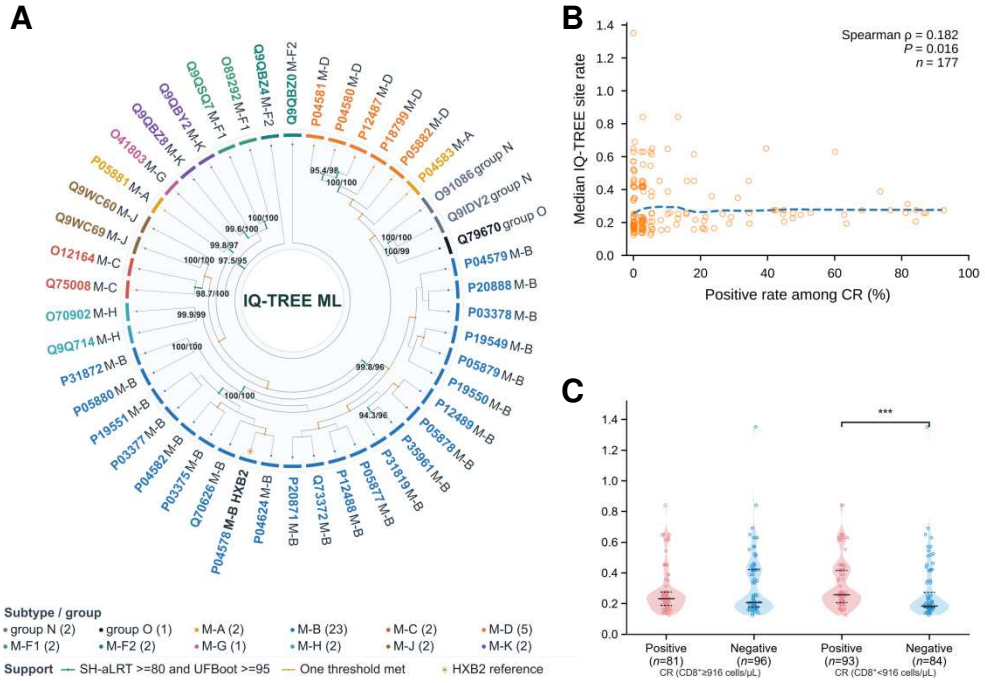

Figure 6: HIV-1 Env phylogeny and evolutionary-rate analysis. (A) Maximum-likelihood phylogeny of 46 HIV-1 Env gp160 sequences; tip colors denote subtype or group, branch labels show SH-aLRT/ultrafast-bootstrap support, and HXB2 is marked as the coordinate reference. (B) Spearman association between peptide-positive rate among CRs and median IQ-TREE site evolutionary rate for 177 HXB2-mapped Env peptides. (C) Median site-rate distributions for antibody-positive and antibody-negative Env peptides within CR ($CD8^+ \geq 916$ cells/μL; 81 positive and 96 negative peptides) and CR ($CD8^+ < 916$ cells/μL; 93 positive and 84 negative peptides); a peptide was classified as positive when EF>1 in at least one participant in the subgroup. Within-subgroup comparisons used two-sided Mann-Whitney U tests. EF: enrichment factor. ***P<0.001.

Tables

Table 1. General characteristics of the NC and CR cohorts (n=76)

Parameters	NC	CR
	(n=38)	**(n=38)**
Age (years)	40.5 (35, 46.25)	39.5 (35.25, 43)
Men, n (%)	38 (100)	38 (100)
Lymphocyte count (cells/µL)	2341 (2052.5, 2759.75)	2320 (1952.5, 2659.75)
T-lymphocyte count (cells/µL)	1639.5 (1445.25, 2027.5)	1644.5 (1441.75, 1958)
$CD4^+$ T-cell count (cells/µL)	950.5 (779.75, 1076.5)	725.5 (652.5, 903.75)**
$CD8^+$ T-cell count (cells/µL)	621.5 (536.25, 793.5)	709 (572.5, 922.25)
$CD4^+$/lymphocyte ratio (%)	39.34 (33.5, 44.57)	35.47 (29.79, 39.23)*
$CD8^+$/lymphocyte ratio (%)	27.24 (24.24, 32.91)	30.07 (25.92, 37.99)*
T-lymphocyte/lymphocyte ratio (%)	73.52 (69.39, 76.96)	73.12 (67.48, 76.28)
$CD4^+/CD8^+$ ratio	1.43 (1.11, 1.81)	1.14 (0.79, 1.46)**

Data are presented as median (Q1, Q3) or n (%). *P<0.05, **P<0.01, and ***P<0.001 versus the NC group. Stars indicate two-sided exact paired Wilcoxon signed-rank tests for continuous variables available in both groups. Sex was a matching factor and was not tested. NC: HIV-negative control; CR: complete immune-reconstitution responder.

Table 2. General characteristics of study participants according to $CD8^+$ T-cell count

Parameters	NC	CR ($CD8^+$<916 cells/μL)	CR ($CD8^+$≥916 cells/μL)	*P* value		
	(n=38)	(n=28)	(n=10)	NC vs CR ($CD8^+$<916 cells/μL)	NC vs CR ($CD8^+$≥916 cells/μL)	CR ($CD8^+$<916 cells/μL) vs CR ($CD8^+$≥916 cells/μL)
Age (years)	40.5 (35, 46.25)	38.5 (35, 43)	41 (38, 44.5)	0.9948	0.6022	0.5277
Men, n (%)	38 (100)	28 (100)	10 (100)	1.0000	1.0000	1.0000
$CD4^+$ T-cell counts at baseline (cells/μL)	—	437 (358, 518)	251.5 (187.5, 413.25)	—	—	0.0088
Viral load at baseline (copies/mL)	—	2.71×10^4 (1.64×10^4, 1.04×10^5)	8.44×10^4 (3.68×10^4, 9.49×10^4)	—	—	0.2138
Age at HIV diagnosis (years)	—	29.5 (28, 33.25)	32.5 (29.25, 36)	—	—	0.3867
Time on ART (months)	—	97 (85.25, 118.75)	103 (91, 120.75)	—	—	0.6305
Days from diagnosis to HIV suppression	—	187.5 (175.5, 397.25)	172.5 (167.25, 177.5)	—	—	0.0129
Lymphocyte counts (cells/μL)	2341 (2052.5, 2759.75)	2130.5 (1902, 2577)	2792 (2511.25, 3182.75)	0.0693	0.0216	0.0017
T lymphocyte counts (cells/μL)	1639.5 (1445.25, 2027.5)	1505 (1330, 1676.75)	2136 (1979.5, 2407.75)	0.0486	0.0020	<0.0001
$CD4^+$ T-cell counts (cells/μL)	950.5 (779.75, 1076.5)	720.5 (645, 907.25)	790 (712, 898.75)	0.0010	0.1589	0.2018
$CD8^+$ T-cell counts (cells/μL)	621.5 (536.25, 793.5)	627.5 (504.25, 716.75)	1198 (1027, 1285.5)	0.5593	<0.0001	<0.0001
CD4/lymphocyte ratio (%)	39.34 (33.50, 44.57)	36.50 (32.22, 39.54)	30.25 (27.13, 33.77)	0.0856	0.0043	0.0299
CD8/lymphocyte ratio (%)	27.24 (24.24, 32.91)	27.07 (24.96, 31.33)	41.10 (37.79, 48.45)	0.7803	<0.0001	<0.0001
T lymphocyte/lymphocyte ratio (%)	73.52 (69.39, 76.96)	70.91 (65.95, 74.94)	79.69 (72.79, 81.18)	0.1967	0.0281	0.0148
CD4/CD8 ratio	1.43 (1.11, 1.81)	1.36 (1.09, 1.54)	0.72 (0.59, 0.87)	0.1922	<0.0001	0.0002

Continuous variables are presented as median (Q1, Q3) and sex as n (%). Pairwise continuous comparisons used two-sided Mann-Whitney U tests. NC: HIV-negative control; CR: complete immune-reconstitution responder; CR ($CD8^+$<916 cells/μL): CD8-low CR; CR ($CD8^+$≥916 cells/μL): CD8-high CR; ART: antiretroviral therapy; —: not applicable.

Supplementary Files

This is a list of supplementary files associated with this preprint. Click to download.

- SupplementaryMaterials.docx